Pyridine based cross-linked chitosan: a biopolymer adsorbent for the green removal of toxic metals from water

Ibraheem Olayiwola Bisiriyu
University of Johannesburg
Reinout Meijboom (rmeijboom@uj.ac.za)
University of Johannesburg https://orcid.org/0000-0003-0901-5690

Research Article

Keywords: selective adsorption, simultaneous adsorption, adsorption energy, DFT

Posted Date: March 12th, 2021

DOI: https://doi.org/10.21203/rs.3.rs-266015/v1

Pyridine based cross-linked chitosan: a biopolymer adsorbent for the green removal of toxic metals from water

*Ibraheem Olayiwola Bisiriyu and Reinout Meijboom**

Department of Chemical Sciences, University of Johannesburg, PO Box 524, Auckland Park, Johannesburg 2006, South Africa.

correspondence: rmeijboom@uj.ac.za

Abstract

Herein we report the green recovery of toxic metals [namely: Cd^{2+}, Cr^{3+}, Mn^{2+}, Pb^{2+}, and Ni^{2+}] from water utilizing a biopolymer: 2,6-pyridine dicarboxylic acid cross-linked chitosan (PDC-CCS) as the adsorbent. Adsorption studies were performed at a previously determined optimum adsorption conditions for Cu(II) [i.e temperature = 30 °C, pH of about 7.5, contact time = 60 mins and initial metal ion concentration of 2.5 mM]. At the RI-PB/def2-SVP level of theory, the Density Functional Theory (DFT) approach has been used to evaluate adsorption energy for metal ions. Selectivity studies were performed at pH 4.20, 5.56, 6.65 and 7.61. While Mn(II), Cd(II) and Ni(II) were strongly adsorbed at higher pH (7.5), Cr(III) and Pb(II) were seen to be strongly adsorbed at lower pH (around 4.0). Selectivity studies revealed that PDC-CCS can be utilized for simultaneous removal of the metals at pH 4.2; selective adsorption of Mn(II) at pH 5.56 as well as simultaneous-selective removal of Ni(II) and Mn(II) near neutral pH. The maximum adsorption limit of PDC-CCS for Mn(II), Cd(II) and Ni(II), were found to be 1258.79, 1118.70 and 829.62 mmol/g respectively. When compared with some relevant previously used adsorbent, PDC-CCS shows an exceptional adsorption capacity. Consequently, a successful biopolymer adsorbent for the treatment of water contaminated by hazardous metals.

Key words: selective adsorption; simultaneous adsorption; adsorption energy; DFT.

Indisputably, contamination of water by heavy metals constitutes major environmental problem owing to their debilitating effect and uneasy complete removal. Chitosan [a biopolymer obtained from chitin (figure 1a)] on the other hand is known for its high adsorption property towards metal ions [1]. Likewise, improvement in the sorption property of chitosan [with incomplete deacetylation (figure 1b), fully deacetylated (figure 1c)] has been made possible through several modifications that utilize the free amino function group in chitosan

[1,2]. Despite the fact that the utilization of chitosan in its modified form for the expulsion of noxious metals from water has pulled in a great deal of interests as of late [3-45], the utilization of pyridine based cross-linked chitosan has not been accounted for as far as we could possibly know. Recently, we reported a new pyridine based cross-linked chitosan (figure 1d) (2,6-pyridine dicarboxylic acid cross-linked chitosan) as a non-toxic biopolymer adsorbent for the recovery of Cu(II) ions from water [46]. In furtherance to this, the pyridine based biopolymer has been utilized in this study in order to extract other toxic metals from water, including; cadmium, chromium, manganese, lead, and nickel with the end goal of investigating/researching the selectivity of this adsorbent with regard to the solution pH and the interaction time of the adsorbent at the optimum temperature and the ideal initial metal ions concentration. Additionally, the Density Functional Theory (DFT) approach has been employed to justify the the adsorbent's adsorption limit/capacity for each of the metals under scrutiny.

The deacetylation degree of chitosan was determined from previous study [46] by ^{1}H NMR spectroscopy using the formulae:

$$\text{DDA} = \left(1 - \frac{I_{CH_3}}{3 \times \sum I_{H_1}}\right) \times 100\% \quad (1) \quad [47]$$

$$\text{DDA} = \left(\frac{I_{H1-GlnN}}{I_{H1-GlnN} + \frac{1}{3} I_{CH3}}\right) \times 100\% \quad (2) \quad [48,49]$$

Where I_{CH_3} depicts the proton integral in –COCH$_3$ group and $\sum I_{H_1} = I_{H1-GlnN}$ this implies the summation of the proton integral attached to the D-glucosamine unit's C1 atom. Chitosan's degree of deacetylation (DDA) was obtained at 96 percent.

In accordance with the updated literature procedure of Sailakshmi et al [50], pyridine-2,6-dicarboxylic acid crosslinked chitosan (PDC-CCS) was prepared and the cross-linking degree was determined using the bradford assay. The presence of pyridine-2,6-dicarboxylic acid in the PDC-CCS was revealed by ^{13}C NMR and UV-visible spectroscopy through peaks due to aromatic carbons and carbonyl carbons. FT-IR confirmed the interaction of the cross-linker with chitosan at the –NH$_2$ functional group. Elemental analysis showed an increase in the C/N ratio after cross-linking indicating a successful incorporation of the crosslinker. The result of the Bradford assay confirmed that the cross-linking is 100% complete. After crosslinking, X-ray diffraction spectroscopy revealed a reduction in the crystallinity of the biomaterial. Thermal analysis suggested a decrease in stability upon cross-linking. N$_2$ adsorption isotherm and SEM

analysis indicated an increased surface area as well as increased porosity of the synthesized cross-linked chitosan [46].

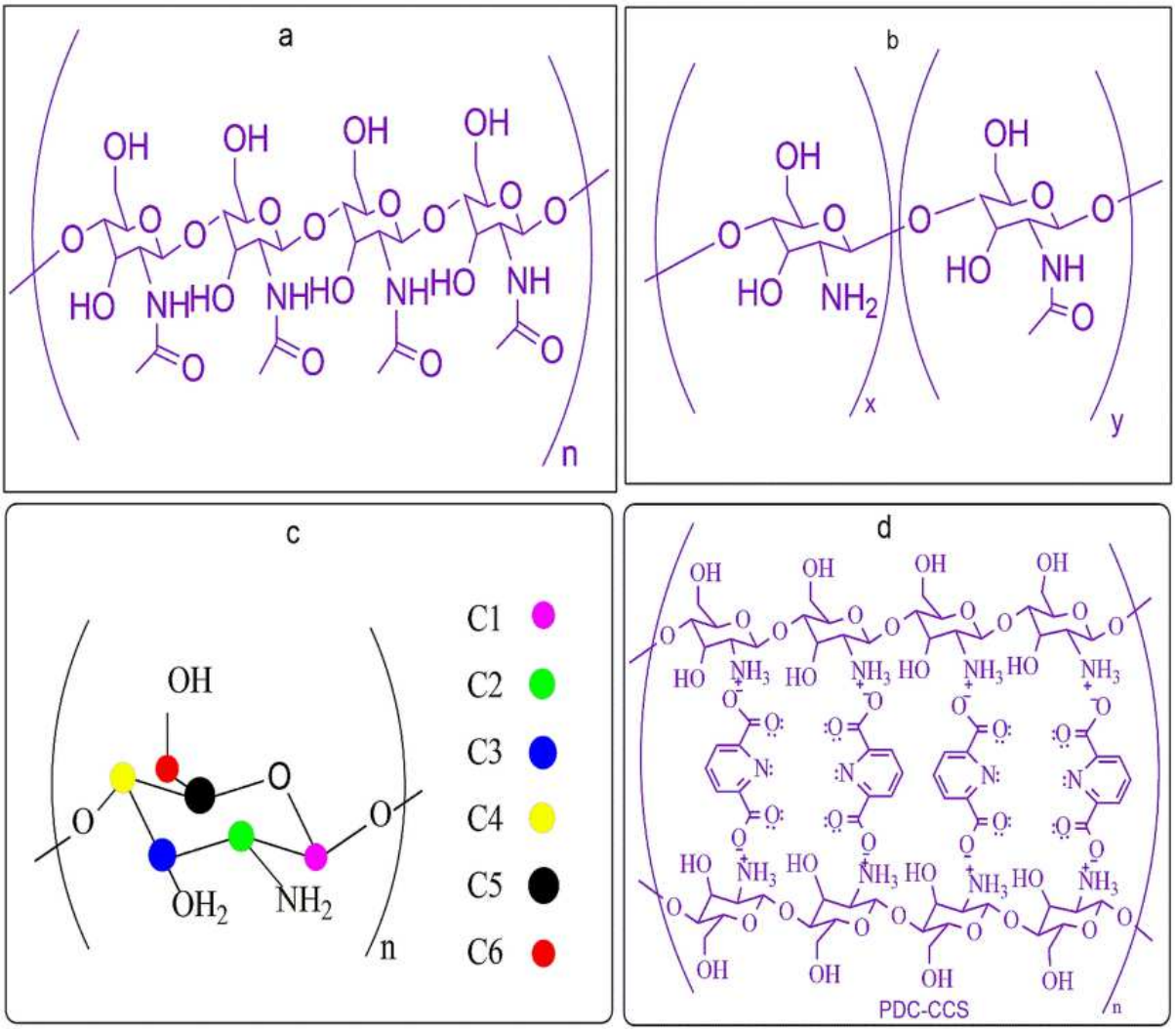

Figure 1: Structure of (a) chitin (b) chitosan (c) fully deacetylated chitosan (d) crosslinked chitosan showing possible binding sites

Following the Thien et al literature approach, we used PDC-CCS from previous research to recover Cu(II) from water. [47]. In addition, to obtain an optimal adsorption state, the impact of temperature, the solution pH, adsorbent time of contact along with initial concentration of Cu(II) ions were examined. In fact, the adsorption limit/capacity Q has been evaluated according to equation 3.

$$Q = \frac{V \times (C_o - C)}{W} \tag{3}$$

Where Q, C and C_o are, individually, the adsorption limit/capacity ($mmolg^{-1}$), the final equilibrium concentration of metal ions ($mmoll^{-1}$) and the initial concentration of metal ions.

Likewise, the solution volume (l) and sorbent mass (g) are V and W, respectively. Additionally, evaluation of the experimental data has been performed with kinetic models (pseudo-first-order and second-order kinetic models according to equation 4 and 5 respectively) and models of Isothermal Adsorption (Langmuir and Freundlich adsorption isotherms according to equation 6 and 7 respectively)

$$ln(q_e - q_t) = lnq_e - \frac{k_1}{2.303}t \tag{4}$$

$$\frac{t}{q_t} = \frac{1}{k_2 q_e^2} + \frac{t}{q_e} \tag{5}$$

$$\frac{C_e}{Q_e} = \left(\frac{1}{K_L q_m}\right) + \left(\frac{C_e}{q_m}\right) \tag{6}$$

$$\frac{C_e}{Q_e} = \left(\frac{1}{K_L q_m}\right) + \left(\frac{C_e}{q_m}\right) \tag{7}$$

Where the quantity of Cu(II) ion adsorbed (mgg^{-1}) at equilibrium and time t is q_e and q_t respectively; The first-order and second-order adsorption rate constants (min^{-1}) are respectively expressed by k_1 and k_2; Ce is the equilibrium Cu(II) ion concentration in solution (mgl^{-1}), whereas the equilibrium adsorption limit/capacity (mgg^{-1}) is denoted as Q_e; for a single-layer coverage (mgg^{-1}), q_m represents the saturated adsorption limit, while k_f, n and K_L are taken as constants. The observed optimum adsorption conditions were: temperature of 30 °C, pH of about 7.5, the initial concentration of Cu(II) ions was found to be 2.5 mM and the contact time was 60 mins. The second-order kinetic model was in good fitness with the experimental adsorption of the Cu(II) ion onto PDC-CCS. Similarly, the Langmuir isothermal adsorption model was adequate for the elucidation of the experimental results. In the same vein, the adsorption process has been shown to be spontaneous and enthalpy driven from the result obtained from the thermodynamic studies of adsorption. In particular, a high value of 2186 mmol/g was obtained for Cu(II) ions as the maximum adsorption limit/capacity of the PDC-CCS. This value was much higher when compared with value obtained from other studies in the literature. Moreover, PDC-CCS could easily be regenerated and reuse for several adsorption cycles. [46].

While we expect the adsorption of other metals [Cd^{2+}, Cr^{3+}, Mn^{2+}, Pb^{2+} and Ni^{2+}] onto the PDC-CCS to follow the same mechanism/model for the recovery of Cu (II), the assessment of the PDC-CCS adsorption potential for each of the metals was carried out under optimum Cu(II) adsorption conditions. Solutions of the metal ions [Cd^{2+}, Cr^{3+}, Mn^{2+}, Pb^{2+} and Ni^{2+}] at the

optimum initial concentration were first prepared by dissolving calculated amount of the salts [$CdCl_2 \cdot H_2O$, $Cr(NO_3)_3 \cdot 9H_2O$, $MnCl_2 \cdot 4H_2O$, $(CH_3COO)_2Pb \cdot 3H_2O$ and $NiCl_2$,] separately in distilled water. The metal ions concentrations in the solutions were determined with Spectro Arcos ICP-OES. To change the pH of the solutions to the optimum pH, sodium hydroxide and hydrogen chloride solutions were added where appropriate. In 25 ml of prepared metal ion solutions, 0.005 g of PDC-CCS was added separately with constant shaking at the optimum temperature and contact time, at some time intervals, a 0.25 ml solution was taken and the concentrations of the metal ions in the samples were again measured. Based on the difference between the initial and final concentration of metal ions in aqueous solutions, the adsorption limit for metal ions was calculated at a given time using equation 3.

The adsorbent selectivity for the metal ions in the solution was examined by first preparing a 25 ml solution mixture of Cd^{2+}, Cr^{3+}, Mn^{2+}, Pb^{2+}, Ni^{2+}, and Cu^{2+} at the said ideal concentration of the metal ions by weighing calculated amount of the respective salts in a graduated vessel and diluting up to the required volume. Aqueous hydrochloric acid/ammonia was used where appropriate to change the solution's pH. Four different solution mixtures of the metal ions were thus prepared with a pH of 4.20, 5.56, 6.65 and 7.61. The initial concentrations of the metal ions were calculated for the four separate solutions using ICP-OES. Thereafter, a 0.005g of the adsorbent (PDC-CCS) was added separately into the four different solutions with continuous shaking at the optimum temperature. Samples from the solutions were taken at intervals of 5, 10, 15, and 20 mins; the concentration of metal ions in the samples was again measured, the capacity of adsorption was calculated, and the selectivity for each metal was examined.

The second-order kinetic model closely suits the adsorption of Cu(II) on the adsorbent (PDC-CCS), thus suggesting a chemisorption in which the Cu(II) ions are mainly adsorbed through complexation by the various donor sites on the adsorbent [46]. The adsorption energy for each of the metal has been estimated by computing the final single point energy (FSE) of the adsorbent, metal ion in solution, adsorbent-metal complexes and H_2O. The chemical structures of the adsorbent, metal ion in solution, adsorbent-metal complex and H_2O were drawn with AVOGADRO and pre-optimized. However, for an easy simulation, the ionic interaction of protonated chitosan with ions of pyridine-2,6-dicarboxylate was replaced with a peptide linkage as the interaction can as well occur through condensation by the elimination of water molecule. The charges on the metal ions were taken into consideration; and where necessary, the spin multiplicities were assigned base on a strong field ligand for the adsorbent-metal and a weak field ligand for the metal ions in solution. Thereafter, geometry optimization of the

chemical structures were performed using ORCA at the RI-PB/def2-SVP level of theory with the aim of obtaining the final single point energies. The adsorption energy (E_{ads}) was calculated as follows:

$$E_{ads} = [E(\text{adsorbent-metal}_{(s)}) + E(nH_2O)] - [E(\text{adsorbent}_{(s)}) + E(\text{metal}_{(aq)})] \quad (8)$$

Where $E(\text{adsorbent-metal}_{(s)})$ is the final single point energy (FSE) of the adsorbent bound metal, $E(nH_2O)$ is the FSE of n molecules of water, $E(\text{adsorbent}_{(s)})$ is the FSE of the adsorbent (PDC-CCS) and $E(\text{metal}_{(aq)})$ is the FSE of metal ion in solution.

The adsorption process is illustrated in scheme 1 where the metal ions are chelated by the O and N donor sites on the adsorbent mainly by the transfer of charge from the adsorbent to the metal ions in solution, as indicated by the NPA charge obtained from Natural bond orbital (NBO) calculations [46]. Figure 2 shows the result obtained when PDC-CCS was used to remove other toxic metals [Cd(II), Cr(III), Mn(II), Pb(II) and Ni(II)] from water at the observed optimum adsorption conditions for Cu(II) while the competitive adsorption capacities and selectivity of PDC-CCS for the metals at pH 4.20, 5.56, 6.65 and 7.61 are shown in figure 3, 4, 5, and 6 respectively. The decrease in adsorbent's capacity of adsorption for the metals as illustrated in figure 2 is as follows: $Ni^{2+} > Cd^{2+} > Mn^{2+} > Pb^{2+} > Cr^{3+}$. However, it should be noted that the 2.5 mM of Pb(II) gave some precipitate of $Pb(OH)_2$ at pH 4.2, the amount of precipitate increases as the pH is increased. Similar observation was seen with 2.5 mM of Cr(III) giving a precipitate of $Cr(OH)_3$ at pH 5.56 and higher. The result of the computational studies and selectivity studies revealed that the PDC-CCS's capacity of adsorption for Pb(II) and Cr(III) would be higher than the result obtained in figure 2 if Pb(II) and Cr(III) were adsorbed at a lower pH (around 4.0). This is evident from the adsorption energies obtained from the computational studies in table 1 [i.e the adsorption energy for Pb(II) is less than Mn(II)] and adsorption capacity obtained from selectivity studies at pH of 4.20 (figure 3). Thus, the optimum adsorption capacity of PDC-CCS for Pb(II) and Cr(III) would be over 859.05 mmol/g and 519.26 mmol/g in the absence of competitive cations as seen in figure 3a and b respectively. Hence, the optimum pH of 7.5 can only be considered for the adsorption of Cd^{2+}, Mn^{2+}, Ni^{2+} and Cu^{2+}.

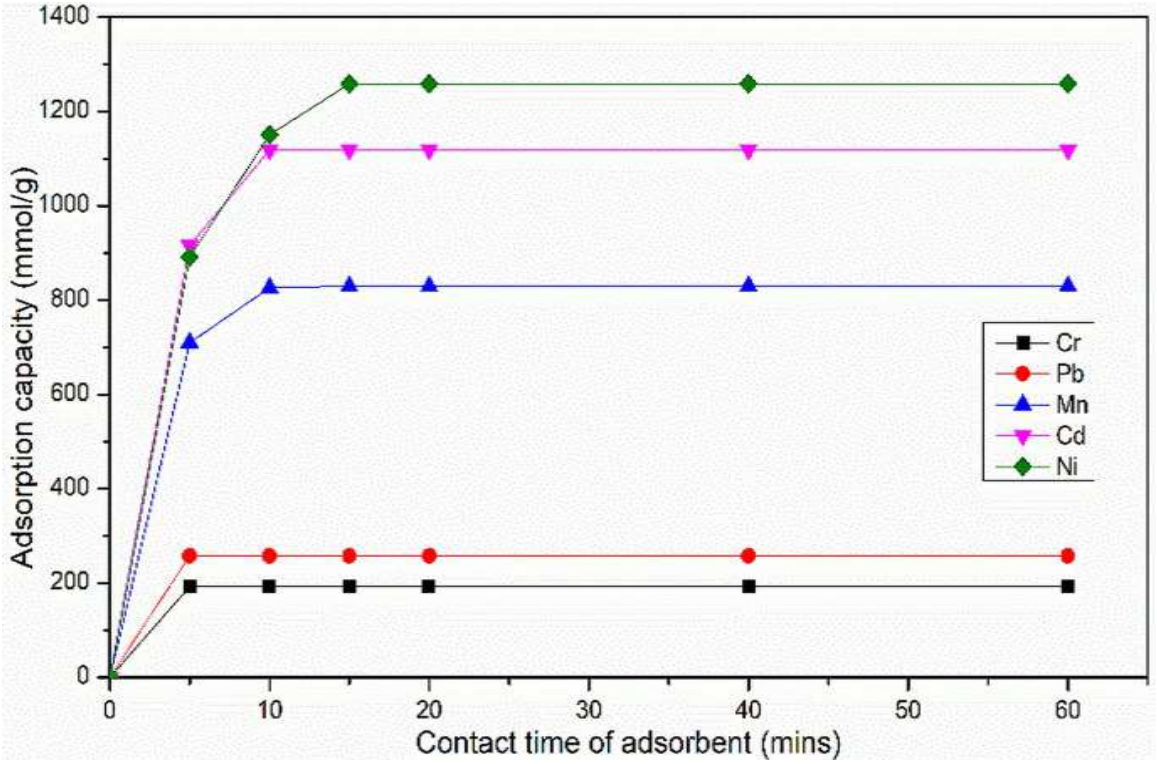

Figure 2: Capacity of adsorption of PDC-CCS for Cr^{3+}, Pb^{2+}, Mn^{2+}, Cd^{2+}, and Ni^{2+} [at 30 °C, pH 7.5, initial metal ion concentration of 2.5 mmol/l]

Table 1: Result of FSE for the adsorbent, metal ions in solution [$metal_{(aq)}$], adsorbent bound-metal [$adsorbent\text{-}metal_{(s)}$], $6H_2O$ and adsorption energy.

$E_{adsorbent(s)}$ (Eh)	$E_{metal(aq)}$ (Eh)	$E_{adsorbent\text{-}metal(s)}$ (Eh)	$6(EH_2O)$ (Eh)	Adsorption energy (Eh)
	Cu(II)			
-3459.0801	-2098.2197	-5099.1858	-458.1648	-0.0508
	Ni(II)			
-3459.0801	-1966.1280	-4967.0907	-458.1648	-0.0474
	Cd(II)			
-3459.0801	-625.5834	-3626.5422	-458.1648	-0.0435
	Pb(II)			
-3459.0801	-650.3730	-3651.2985	-458.1648	-0.0103
	Mn(II)			
-3459.0801	-1608.8333	-4609.751	-458.1648	-0.0024

	Cr(III)			
-3459.0801	-1501.6064	-4502.5*	-458.1648	0.0217

*: Optimization energy not converged after 3000 iterations

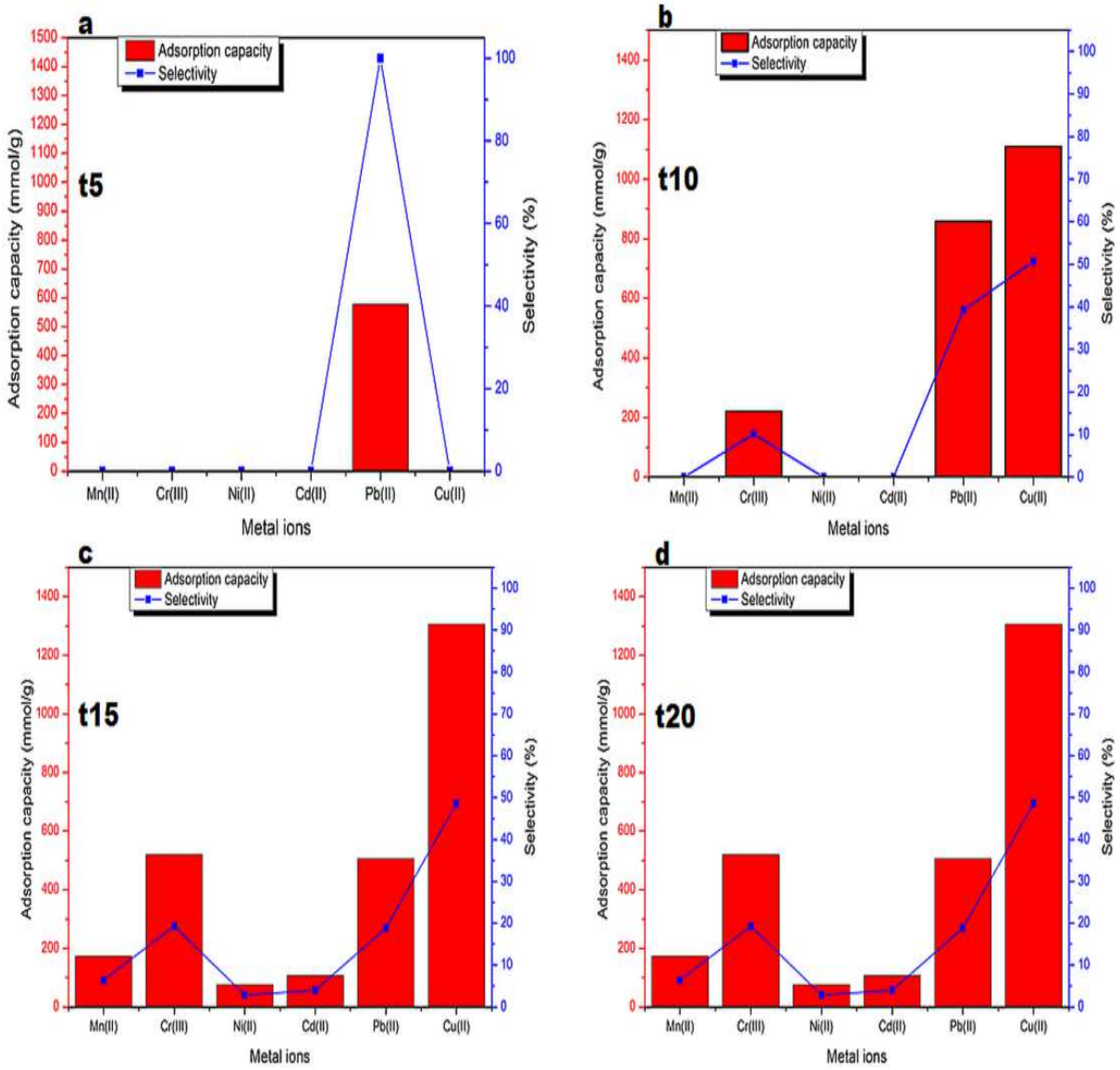

Figure 3: Competitive adsorption capacities and selectivity of PDC-CCS at pH 4.2 for Mn^{2+}, Cr^{3+}, Ni^{2+}, Cd^{2+}, Pb^{2+}, and Cu^{2+} within; (a) five mins (b) ten mins (c) fifteen mins and (d) twenty mins.

Additionally, the selectivity studies show that the adsorbent (PDC-CCS) has the tendency to adsorb all the competing metal ions within 15 minutes of contact time at a pH of 4.2 (figure 3). The capacity of adsorption and adsorbent's selectivity towards the metal ions are in the following order: $Cu^{2+} > Pb^{2+} > Cr^{3+} > Mn^{2+} > Cd^{2+} > Ni^{2+}$. However, at pH 5.56 (figure 4), the tendency of the adsorbent to adsorb the metal ions in solution decreases but with high selectivity (100%) towards Mn(II). The observed reduction in adsorption capacity at the pH of 5.56 may be due to the strong competition among the metal ions for uptake by the adsorbent.

In essence, as one metal ion is adsorbed, it is replaced by another metal ion; the process continues until an equilibrium is attained when small amount of Mn(II) is successfully adsorbed without replacement after 15 minutes of contact time.

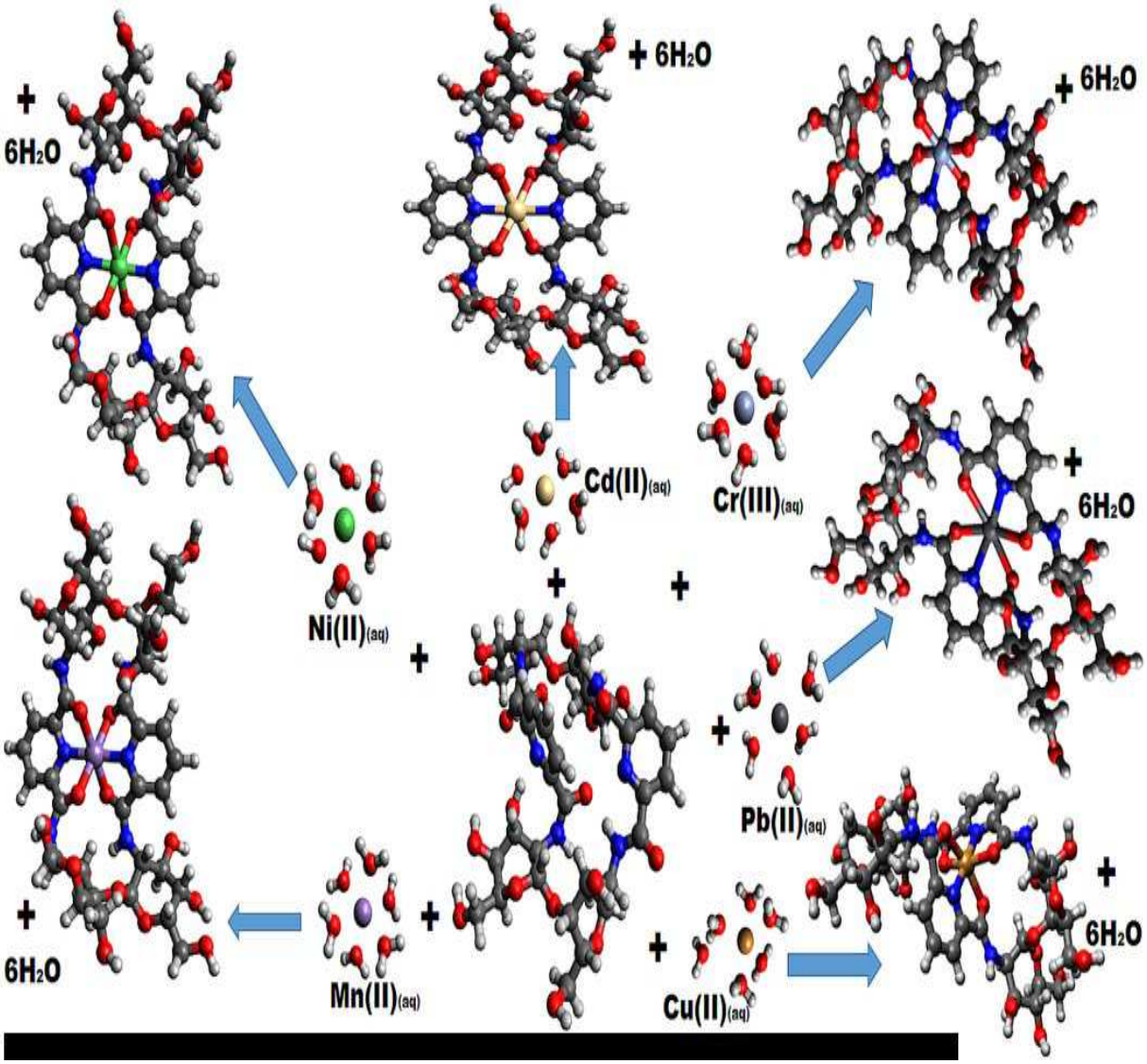

Scheme 1: Adsorption process of the metal ions [Mn^{2+}, Cr^{3+}, Ni^{2+}, Cd^{2+}, Pb^{2+} and Cu^{2+}] on the adsorbent [PDC-CCS] via chelation/complexation

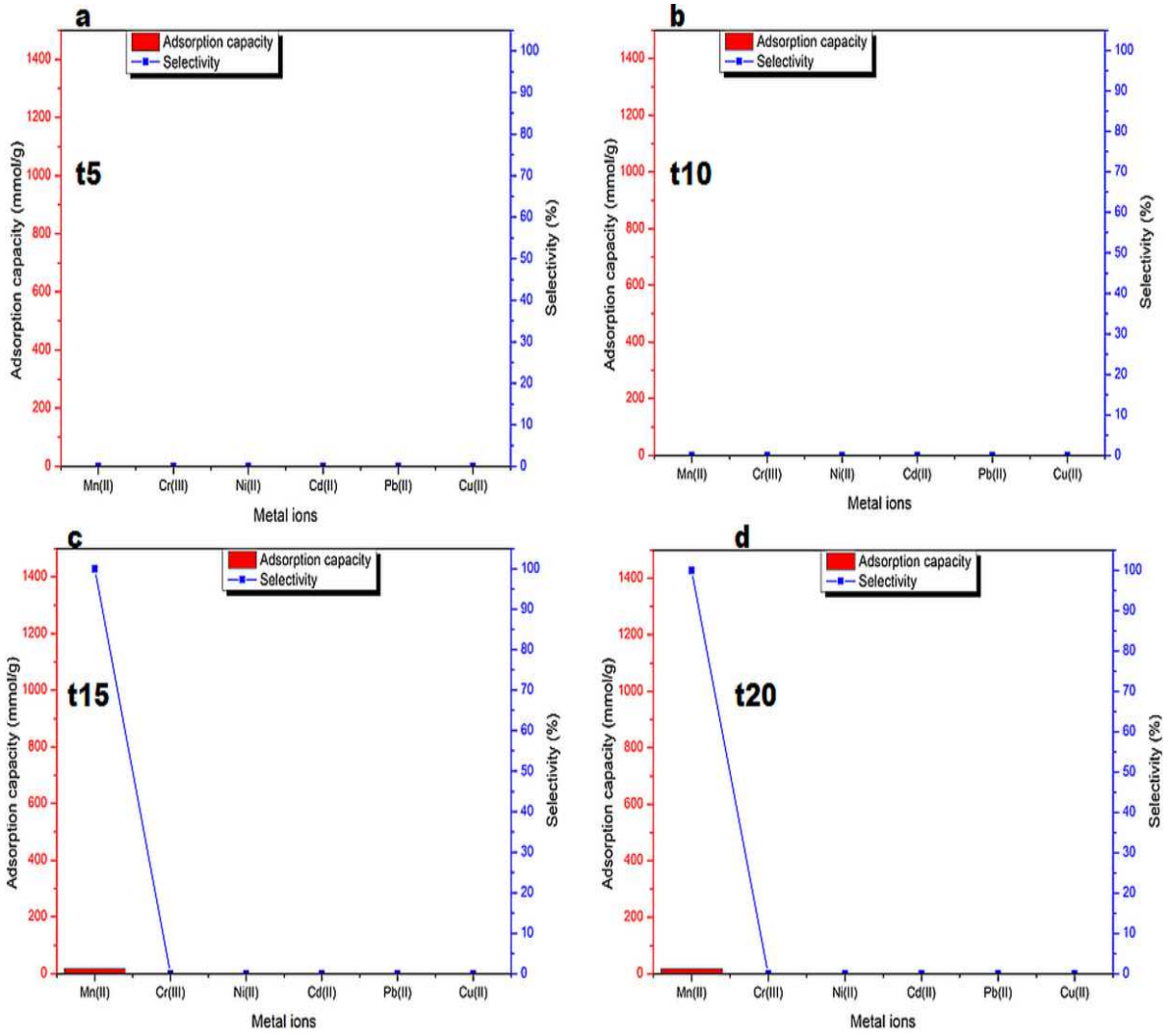

Figure 4: Competitive adsorption capacities and selectivity of PDC-CCS at pH 5.6 for Mn^{2+}, Cr^{3+}, Ni^{2+}, Cd^{2+}, Pb^{2+}, and Cu^{2+} within; (a) five mins (b) ten mins (c) fifteen mins and (d) twenty mins.

Table 2: Comparison between PDC-CCS adsorption capability and some previously recorded relevant adsorbents

Author/year	Adsorbent	Adsorption Capacity	Reference
	Ni(II)		
Cuiping Wang et al. (2012)	Tourmaline	13.10 mg/g	[51]
Guanhao Liu et al. (2009)	Mg-Al Hydrotalcites Intercalated by ethylenediaminetetraacetic acid	108.20 mg/g	[52]

Debashis kundu et al. (2019)	B-Cyclodextrin-Cellulose/Hemi cellulose-Based Hydrogels	15.93 mg/g	[53]
Liping Fang et al. (2015)	LDH – HA	480.40 mg/g	[54]
	LDH – FA	290.60 mg/g	
Sayed Zia Mohammadi et al. (2014)	Activated Carbon from *Glycyrrhiza glabra* residue	166.70 mg/g	[55]
Eveliina Repo et al. (2009)	Silica gel functionalized with EDTA	21.60 mg/g	[56]
	DTPA-modified silica gel	16.70 mg/g	
Vinod Kumar Gupta et al. (2014)	Scrap tyre	25 mg/g	[57]
Wei Shen et al. (2019)	Alginate modified graphitic carbon nitride hydrogels	306.30 mg/g	[58]
Dawodu and Akpomie (2014)	Nigerian Kaolinite clay	166.67 mg/g	[59]
Ibraheem and Reinout (2021)	PDC-CCS	1258.79 mmol/g	This work
	Cd(II)		
Cuiping Wang et al. (2012)	Tourmaline	25.19 mg/g	[51]
Debashis kundu et al. (2019)	B-Cyclodextrin-Cellulose/Hemi cellulose-Based Hydrogels	24.66 mg/g	[53]
Jayabrata and Samit	Biocomposite Hydrogel	193.90 mg/g	[60]
Rashi Gusain et al. (2019)	(M_oS)/thiol functionalized multiwalled carbon nanotube (SH-MWCNT)	66.60 mg/g	[61]
Diana Cholico-Gonzalez et al. (2020)	Agave Bagasse	93.14 mg/g	[62]
Xiong Yang et al. (2020)	Birnessite	239.7 mg/g	[63]
Pu Yang et al. (2020)	Ion-imprinted polymers	41.212 mg/g	[64]

Fudong Wang et al. (2019)	Straw Cellulose Hydrogel Beads ($SCHB_s$)	95.62 mg/g	[65]
Jianhua Guo et al. (2019)	HA/Fe-Mn Oxides-loaded biochar composite (HFMB)	67.11 mg/g	[66]
Emmanuel F. Olasehinde et al. (2019)	Onion skin	21.28 mg/g	[67]
Ibraheem and Reinout (2021)	PDC-CCS	1118.70 mmol/g	This work
	Mn(II)		
Han Yan et al. (2014)	Magnetic grapheme oxide	16.5 mg/g	[68]
Dawodu and Akpomie (2014)	Nigerian Kaolinite clay	111.11 mg/g	[59]
Z. Abdeen et al. (2015)	Polyvinyl alcohol/Chitosan (PVA/CS)	10.515 mg/g	[69]
Yong Liu et al. (2017)	Magnetic Fe_3O_4 nano-particles	36.81 mg/g	[70]
Xiangbing Zhu et al. (2016)	Diethylenetriamine-functionalized carbon nanotubes dispersed in grapheme oxide colloids	9.5 mg/g	[71]
Mingjie Huang et al. (2019)	Layered doubled hydroxide intercalated with diethylene triamine pentaacetic acid (LDH_s-DTPA)	83.5 mg/g	[72]
	LDH_s-EDTA	44.4 mg/g	
	LDH_s-Oxalate	21.6 mg/g	
	LDH_s	28.8 mg/g	
Zhangxiang Lin et al. (2020)	Zeolite	8.6 mg/g	[73]
Ramin Mohammadi et al. (2019)	Alginate-Combusted coal gangue composite	64.29 mg/g	[74]
Seung-Moklee et al. (2009)	Manganese-coated sand sample (MCS)	59.34 mg/g	[75]
Ibraheem and Reinout (2021)	PDC-CCS	829.62 mmol/g	This work

Similarly, the selectivity of PDC-CCS shifted towards Ni(II) and Mn(II) near neutral pH (i.e pH 6.65 and 7.61 as seen in figure 5 and 6 respectively). A small amount of Cr(III) was initially adsorbed but was replaced within 15 minutes of contact time. However, PDC-CCS adsorbed more Ni(II) than Mn(II) at both pH values.

Interestingly, PDC-CCS shows exceptional adsorption capacity towards metal ions compared to some of the applicable adsorbents previously published as shown in table 2.

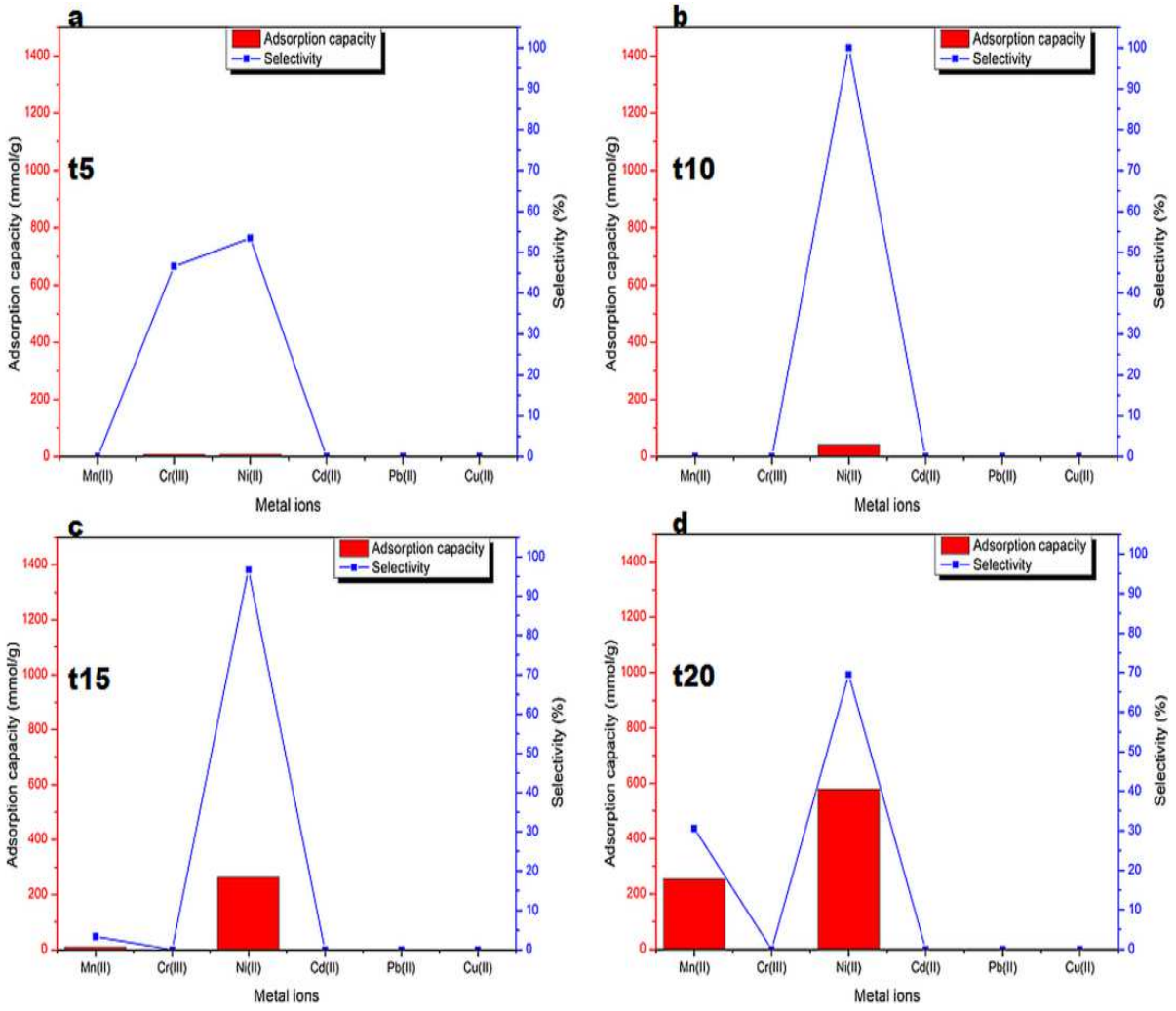

Figure 5: Competitive adsorption capacities and selectivity of PDC-CCS at pH 6.65 for Mn^{2+}, Cr^{3+}, Ni^{2+}, Cd^{2+}, Pb^{2+}, and Cu^{2+} within; (a) five mins (b) ten mins (c) fifteen mins and (d) twenty mins.

Conclusion

The adsorption of Cd^{2+}, Cr^{3+}, Mn^{2+}, Pb^{2+} and Ni^{2+} utilizing 2,6-pyridinedicarboxylic acid crosslinked chitosan (PDC-CCS) has been discussed. The capacity of adsorption by PDC-CCS was investigated at pH 7.5 while adsorption selectivities were examined at pH 4.2, 5.56, 6.65 and 7.61. Density functional theory approach has been used to support the trend in adsorption

capacities of PDC-CCS for the metal ions. Results obtained indicate that PDC-CCS is a novel biopolymer adsorbent which can be employed for the simultaneous removal of toxic metals and selective removal of Mn(II) from water.

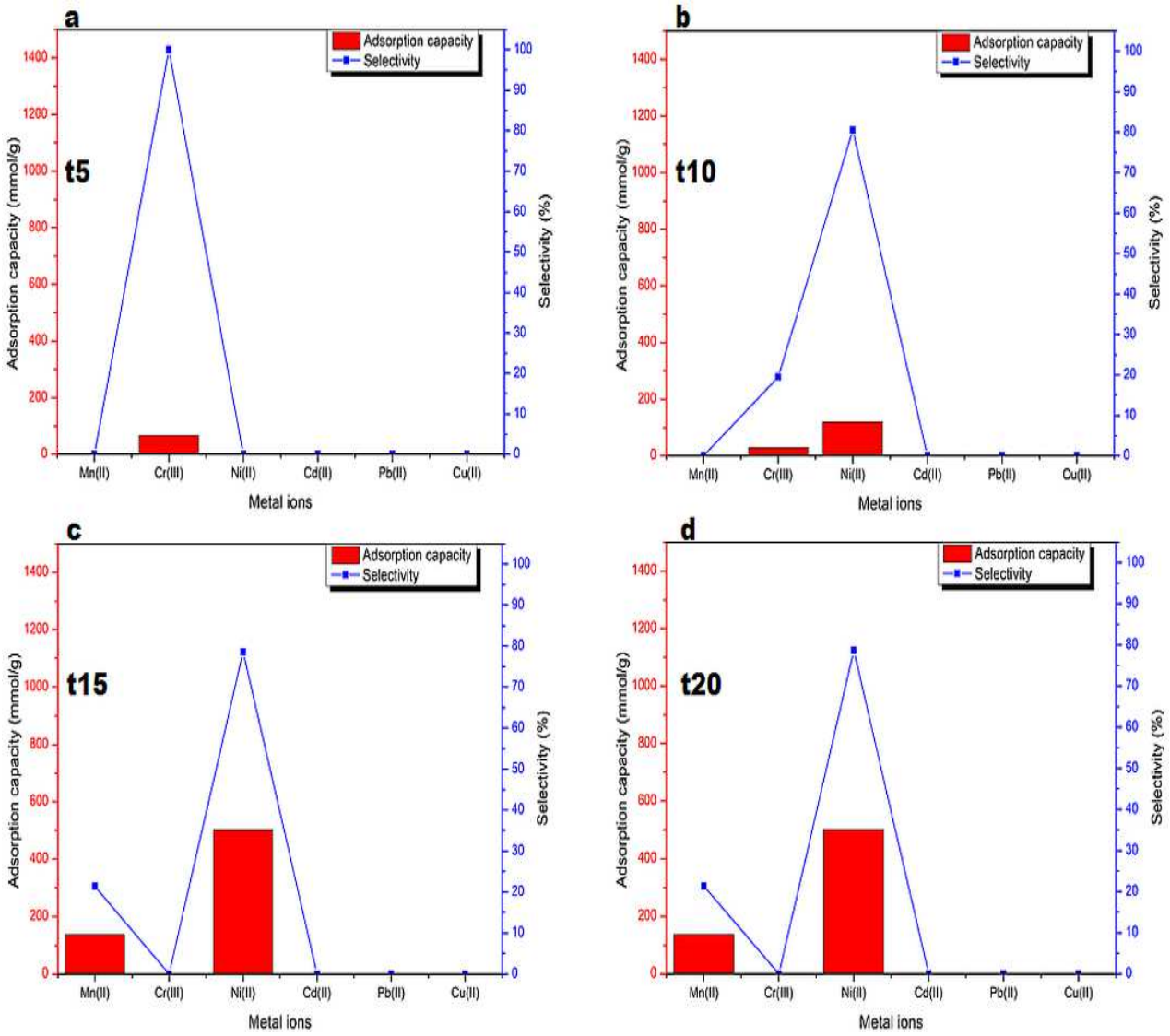

Figure 6: Competitive adsorption capacities and selectivity of PDC-CCS at pH 7.61 for Mn^{2+}, Cr^{3+}, Ni^{2+}, Cd^{2+}, Pb^{2+}, and Cu^{2+} within; (a) five mins (b) ten mins (c) fifteen mins and (d) twenty mins.

Conflicts of interest

There are no disputes to report.

Acknowledgement

The financial support provided for this research from The World Academy of Sciences (TWAS) in partnership with the National Research Foundation (NRF) is hereby recognized. The views expressed and the conclusions drawn, are those of the author and are not inherently attributable to the NRF-TWAS.

Reference List

[1] K.R. Krishnapriya, M. Kandaswamy, A new chitosan biopolymer derivative as metal-complexing agent: synthesis, characterization, and metal(II) ion adsorption studies, Carbohydrate Research. 345 (2010) 2013-2022.

[2] C.A. Rodrigues, M.C.M. Laranjeira, V.T. de Fávere, E. Stadler, Interaction of Cu(II) on N-(2-pyridylmethyl) and N-(4-pyridylmethyl) chitosan, Polymer. 39 (1998) 5121-5126.

[3] W.S. Wan Ngah, L.C. Teong, M.A.K.M. Hanafiah, Adsorption of dyes and heavy metal ions by chitosan composites: A review, Carbohydrate Polymers. 83 (2011) 1446-1456.

[4] A.K. Bajpai, Facile preparation of ionotropically crosslinked chitosan-alginate nanosorbents by water-in-oil (W/O) microemulsion technique: Optimization and study of arsenic (V) removal, Journal of Water Process Engineering. 32 (2019) 100920.

[5] P. Baroni, R.S. Vieira, E. Meneghetti, da Silva, M. G. C., M.M. Beppu, Evaluation of batch adsorption of chromium ions on natural and crosslinked chitosan membranes, J. Hazard. Mater. 152 (2008) 1155-1163.

[6] A. Chen, S. Liu, C. Chen, C. Chen, Comparative adsorption of Cu (II), Zn (II), and Pb (II) ions in aqueous solution on the crosslinked chitosan with epichlorohydrin, J. Hazard. Mater. 154 (2008) 184-191.

[7] A. Chen, C. Yang, C. Chen, C. Chen, C. Chen, The chemically crosslinked metal-complexed chitosans for comparative adsorptions of Cu(II), Zn(II), Ni(II) and Pb(II) ions in aqueous medium, J. Hazard. Mater. 163 (2009) 1068-1075.

[8] M.L.P. Dalida, A.F.V. Mariano, C.M. Futalan, C. Kan, W. Tsai, M. Wan, Adsorptive removal of Cu(II) from aqueous solutions using non-crosslinked and crosslinked chitosan-coated bentonite beads, Desalination. 275 (2011) 154-159.

[9] S. Dandil, D. Akin Sahbaz, C. Acikgoz, Adsorption of Cu(II) ions onto crosslinked chitosan/Waste Active Sludge Char (WASC) beads: Kinetic, equilibrium, and thermodynamic study, Int. J. Biol. Macromol. 136 (2019) 668-675.

[10] S. Ding, X. Zhang, X. Feng, Y. Wang, S. Ma, Q. Peng, W. Zhang, Synthesis of N,N′-diallyl dibenzo 18-crown-6 crown ether crosslinked chitosan and their adsorption properties for metal ions, React Funct Polym. 66 (2006) 357-363.

[11] H. Ge, T. Hua, X. Chen, Selective adsorption of lead on grafted and crosslinked chitosan nanoparticles prepared by using Pb2+ as template, J. Hazard. Mater. 308 (2016) 225-232.

[12] H. Ge, T. Hua, Synthesis and characterization of poly(maleic acid)-grafted crosslinked chitosan nanomaterial with high uptake and selectivity for Hg(II) sorption, Carbohydr. Polym. 153 (2016) 246-252.

[13] P. Gogoi, A.J. Thakur, R.R. Devi, B. Das, T.K. Maji, A comparative study on sorption of arsenate ions from water by crosslinked chitosan and crosslinked chitosan/MMT nanocomposite, Journal of Environmental Chemical Engineering. 4 (2016) 4248-4257.

[14] B. Hastuti, Y. Santrinitas, Swelling and Crosslinked Formaldehyde Chitosan as Adsorbent for Metal Ion Cu (II), Materials Science Forum. 890 (2017) 171-175.

[15] C. Jiang, X. Wang, G. Wang, C. Hao, X. Li, T. Li, Adsorption performance of a polysaccharide composite hydrogel based on crosslinked glucan/chitosan for heavy metal ions, Composites Part B: Engineering. 169 (2019) 45-54.

[16] T. Kameda, R. Honda, S. Kumagai, Y. Saito, T. Yoshioka, Adsorption of Cu2+ and Ni2+ by tripolyphosphate-crosslinked chitosan-modified montmorillonite, Journal of Solid State Chemistry. 277 (2019) 143-148.

[17] M. Kumar, B.P. Tripathi, V.K. Shahi, Crosslinked chitosan/polyvinyl alcohol blend beads for removal and recovery of Cd(II) from wastewater, J. Hazard. Mater. 172 (2009) 1041-1048.

[18] R. Laus, T.G. Costa, B. Szpoganicz, V.T. Fávere, Adsorption and desorption of Cu(II), Cd(II) and Pb(II) ions using chitosan crosslinked with epichlorohydrin-triphosphate as the adsorbent, J. Hazard. Mater. 183 (2010) 233-241.

[19] Y. Li, M. Li, J. Zhang, X. Xu, Adsorption properties of the double-imprinted electrospun crosslinked chitosan nanofibers, Chinese Chemical Letters. 30 (2019) 762-766.

[20] Manasi, V. Rajesh, N. Rajesh, An indigenous Halomonas BVR1 strain immobilized in crosslinked chitosan for adsorption of lead and cadmium, Int. J. Biol. Macromol. 79 (2015) 300-308.

[21] S. Mallakpour, E. Khadem, Linear and nonlinear behavior of crosslinked chitosan/N-doped graphene quantum dot nanocomposite films in cadmium cation uptake, Sci. Total Environ. 690 (2019) 1245-1253.

[22] J.S. Marques, M.R. Pereira, A. Sotto, J.M. Arsuaga, Removal of aqueous copper(II) by using crosslinked chitosan films, Reactive and Functional Polymers. 134 (2019) 31-39.

[23] J. Mei, H. Zhang, Z. Li, H. Ou, A novel tetraethylenepentamine crosslinked chitosan oligosaccharide hydrogel for total adsorption of Cr(VI), Carbohydr. Polym. 224 (2019) 115154.

[24] L. Midya, R. Das, M. Bhaumik, T. Sarkar, A. Maity, S. Pal, Removal of toxic pollutants from aqueous media using poly (vinyl imidazole) crosslinked chitosan synthesised through microwave assisted technique, J. Colloid Interface Sci. 542 (2019) 187-197.

[25] W.S.W. Ngah, S. Fatinathan, Pb(II) biosorption using chitosan and chitosan derivatives beads: Equilibrium, ion exchange and mechanism studies, Journal of Environmental Sciences. 22 (2010) 338-346.

[26] M.L. Nguyen, R. Juang, Modification of crosslinked chitosan beads with histidine and Saccharomyces cerevisiae for enhanced Ni(II) biosorption, Journal of the Taiwan Institute of Chemical Engineers. 56 (2015) 96-102.

[27] P.A. Nishad, A. Bhaskarapillai, S. Velmurugan, Nano-titania-crosslinked chitosan composite as a superior sorbent for antimony (III) and (V), Carbohydr. Polym. 108 (2014) 169-175.

[28] A.A. Radwan, F.K. Alanazi, I.A. Alsarra, Microwave irradiation-assisted synthesis of a novel crown ether crosslinked chitosan as a chelating agent for heavy metal ions (M(+n)), Molecules (Basel, Switzerland). 15 (2010) 6257-6268.

[29] Rahmi, Lelifajri, R. Nurfatimah, Preparation of polyethylene glycol diglycidyl ether (PEDGE) crosslinked chitosan/activated carbon composite film for Cd2+ removal, Carbohydr. Polym. 199 (2018) 499-505.

[30] A. Ramesh, H. Hasegawa, W. Sugimoto, T. Maki, K. Ueda, Adsorption of gold(III), platinum(IV) and palladium(II) onto glycine modified crosslinked chitosan resin, Bioresource Technology. 99 (2008) 3801-3809.

[31] S.P. Ramnani, S. Sabharwal, Adsorption behavior of Cr(VI) onto radiation crosslinked chitosan and its possible application for the treatment of wastewater containing Cr(VI), Reactive and Functional Polymers. 66 (2006) 902-909.

[32] G. Sharma, M. Naushad, A.H. Al-Muhtaseb, A. Kumar, M.R. Khan, S. Kalia, Shweta, M. Bala, A. Sharma, Fabrication and characterization of chitosan-crosslinked-poly(alginic acid) nanohydrogel for adsorptive removal of Cr(VI) metal ion from aqueous medium, Int. J. Biol. Macromol. 95 (2017) 484-493.

[33] A. Shekhawat, S. Kahu, D. Saravanan, R. Jugade, Synergistic behaviour of ionic liquid impregnated sulphate-crosslinked chitosan towards adsorption of Cr(VI), Int. J. Biol. Macromol. 80 (2015) 615-626.

[34] T. Shi, D. Yang, H. Yang, J. Ye, Q. Cheng, Preparation of chitosan crosslinked modified silicon material and its adsorption capability for chromium(VI), Appl. Clay. Sci. 142 (2017) 100-108.

[35] S. Sun, L. Wang, A. Wang, Adsorption properties of crosslinked carboxymethyl-chitosan resin with Pb(II) as template ions, J. Hazard. Mater. 136 (2006) 930-937.

[36] Z.A. Sutirman, M.M. Sanagi, K.J. Abd Karim, W.A. Wan Ibrahim, Preparation of methacrylamide-functionalized crosslinked chitosan by free radical polymerization for the removal of lead ions, Carbohydr. Polym. 151 (2016) 1091-1099.

[37] Z.A. Sutirman, M.M. Sanagi, J. Abd Karim, A. Abu Naim, W.A. Wan Ibrahim, New crosslinked-chitosan graft poly(N-vinyl-2-pyrrolidone) for the removal of Cu(II) ions from aqueous solutions, Int. J. Biol. Macromol. 107 (2018) 891-897.

[38] V.N. Tirtom, A. Dinçer, S. Becerik, T. Aydemir, A. Çelik, Comparative adsorption of Ni(II) and Cd(II) ions on epichlorohydrin crosslinked chitosan–clay composite beads in aqueous solution, Chem. Eng. J. 197 (2012) 379-386.

[39] M. Vakili, S. Deng, T. Li, W. Wang, W. Wang, G. Yu, Novel crosslinked chitosan for enhanced adsorption of hexavalent chromium in acidic solution, Chem. Eng. J. 347 (2018) 782-790.

[40] H.L. Vasconcelos, T.P. Camargo, N.S. Gonçalves, A. Neves, M.C.M. Laranjeira, V.T. Fávere, Chitosan crosslinked with a metal complexing agent: Synthesis, characterization and copper(II) ions adsorption, React Funct Polym. 68 (2008) 572-579.

[41] F.C. Vicentini, T.A. Silva, A. Pellatieri, B.C. Janegitz, O. Fatibello-Filho, R.C. Faria, Pb(II) determination in natural water using a carbon nanotubes paste electrode modified with crosslinked chitosan, Microchemical Journal. 116 (2014) 191-196.

[42] R.S. Vieira, M.M. Beppu, Interaction of natural and crosslinked chitosan membranes with Hg(II) ions, Colloids Surf. Physicochem. Eng. Aspects. 279 (2006) 196-207.

[43] R.S. Vieira, M.L.M. Oliveira, E. Guibal, E. Rodríguez-Castellón, M.M. Beppu, Copper, mercury and chromium adsorption on natural and crosslinked chitosan films: An XPS investigation of mechanism, Colloids Surf. Physicochem. Eng. Aspects. 374 (2011) 108-114.

[44] Y. Yan, G. Yuvaraja, C. Liu, L. Kong, K. Guo, G.M. Reddy, G.V. Zyryanov, Removal of Pb(II) ions from aqueous media using epichlorohydrin crosslinked chitosan Schiff's base@Fe3O4 (ECCSB@Fe3O4), International Journal of Biological Macromolecules. 117 (2018) 1305-1313.

[45] N. Zhang, H. Zhang, R. Li, Y. Xing, Preparation and adsorption properties of citrate-crosslinked chitosan salt microspheres by microwave assisted method, Int. J. Biol. Macromol. (2019).

[46] I.O. Bisiriyu, R. Meijboom, Adsorption of Cu(II) ions from aqueous solution using pyridine-2,6-dicarboxylic acid crosslinked chitosan as a green biopolymer adsorbent, Int. J. Biol. Macromol. 165 (2020) 2484-2493.

[47] T. DT, NT, An and NT Hoa, Preparation of Fully Deacetylated Chitosan for Adsorption of Hg(II) Ion from Aqueous Solution, Chemical Sciences Journal. 6 (2015) 95.

[48] Renata Czechowska-Biskup, Diana Jarosińska, Bożena Rokita, Piotr Ulański, Janusz M. Rosiak, Determination of degree of deacetylation of chitosan - comparision of methods, Progress on Chemistry. 12 (2012) 5-20.

[49] T. Wu, S. Zivanovic, Determination of the degree of acetylation (DA) of chitin and chitosan by an improved first derivative UV method, Carbohydrate Polymers. 73 (2008) 248-253.

[50] G. Sailakshmi, T. Mitra, S. Chatterjee, A. Gnanamani, Engineering Chitosan Using α, ω-Dicarboxylic Acids—An Approach to Improve the Mechanical Strength and Thermal Stability, Journal of Biomaterials and Nanobiotechnology. 4 (2013) 151-164.

[51] C. Wang, J. Liu, Z. Zhang, B. Wang, H. Sun, Adsorption of Cd(II), Ni(II), and Zn(II) by Tourmaline at Acidic Conditions: Kinetics, Thermodynamics, and Mechanisms, Industrial & Engineering Chemistry Research. 51 (2012) 4397-4406.

[52] G. Liu, J. Yang, X. Xu, Z. He, Mg–Al Hydrotalcites Intercalated by Ethylenediaminetetraacetic Acid for Ni(II) Removal from Aqueous Solution, Journal of Chemical & Engineering Data. 64 (2019) 5838-5846.

[53] D. Kundu, S.K. Mondal, T. Banerjee, Development of β-Cyclodextrin-Cellulose/Hemicellulose-Based Hydrogels for the Removal of Cd(II) and Ni(II): Synthesis, Kinetics, and Adsorption Aspects, Journal of Chemical & Engineering Data. 64 (2019) 2601-2617.

[54] L. Fang, W. Li, H. Chen, F. Xiao, L. Huang, P.E. Holm, H.C.B. Hansen, D. Wang, Synergistic effect of humic and fulvic acids on Ni removal by the calcined Mg/Al layered double hydroxide, RSC Advances. 5 (2015) 18866-18874.

[55] S.Z. Mohammadi, H. Hamidian, Z. Moeinadini, High surface area-activated carbon from Glycyrrhiza glabra residue by ZnCl2 activation for removal of Pb(II) and Ni(II) from water samples, Journal of Industrial and Engineering Chemistry. 20 (2014) 4112-4118.

[56] E. Repo, T.A. Kurniawan, J.K. Warchol, M.E.T. Sillanpää, Removal of Co(II) and Ni(II) ions from contaminated water using silica gel functionalized with EDTA and/or DTPA as chelating agents, Journal of Hazardous Materials. 171 (2009) 1071-1080.

[57] V.K. Gupta, Suhas, A. Nayak, S. Agarwal, M. Chaudhary, I. Tyagi, Removal of Ni (II) ions from water using scrap tire, Journal of Molecular Liquids. 190 (2014) 215-222.

[58] W. Shen, Q. An, Z. Xiao, S. Zhai, J. Hao, Y. Tong, Alginate modified graphitic carbon nitride composite hydrogels for efficient removal of Pb(II), Ni(II) and Cu(II) from water, International Journal of Biological Macromolecules. (2019).

[59] F.A. Dawodu, K.G. Akpomie, Simultaneous adsorption of Ni(II) and Mn(II) ions from aqueous solution unto a Nigerian kaolinite clay, Journal of Materials Research and Technology. 3 (2014) 129-141.

[60] J. Maity, S.K. Ray, Competitive Removal of Cu(II) and Cd(II) from Water Using a Biocomposite Hydrogel, The Journal of Physical Chemistry B. 121 (2017) 10988-11001.

[61] R. Gusain, N. Kumar, E. Fosso-Kankeu, S.S. Ray, Efficient Removal of Pb(II) and Cd(II) from Industrial Mine Water by a Hierarchical MoS2/SH-MWCNT Nanocomposite, ACS Omega. 4 (2019) 13922-13935.

[62] D. Cholico-González, N. Ortiz Lara, A.M. Fernández Macedo, J. Chavez Salas, Adsorption Behavior of Pb(II), Cd(II), and Zn(II) onto Agave Bagasse, Characterization, and Mechanism, ACS omega. 5 (2020) 3302-3314.

[63] X. Yang, Q. Peng, L. Liu, W. Tan, G. Qiu, C. Liu, Z. Dang, Synergistic adsorption of Cd(II) and As(V) on birnessite under electrochemical control, Chemosphere. 247 (2020) 125822.

[64] P. Yang, H. Cao, D. Mai, T. Ye, X. Wu, M. Yuan, J. Yu, F. Xu, A novel morphological ion imprinted polymers for selective solid phase extraction of Cd(II): Preparation, adsorption properties and binding mechanism to Cd(II), Reactive and Functional Polymers. 151 (2020) 104569.

[65] F. Wang, J. Li, Y. Su, Q. Li, B. Gao, Q. Yue, W. Zhou, Adsorption and recycling of Cd(II) from wastewater using straw cellulose hydrogel beads, Journal of Industrial and Engineering Chemistry. 80 (2019) 361-369.

[66] J. Guo, C. Yan, Z. Luo, H. Fang, S. Hu, Y. Cao, Synthesis of a novel ternary HA/Fe-Mn oxides-loaded biochar composite and its application in cadmium(II) and arsenic(V) adsorption, Journal of Environmental Sciences. 85 (2019) 168-176.

[67] E.F. Olasehinde, A.V. Adegunloye, M.A. Adebayo, A.A. Oshodi, Cadmium (II) Adsorption from Aqueous Solutions Using Onion Skins, Water Conservation Science and Engineering. (2019).

[68] H. Yan, H. Li, X. Tao, K. Li, H. Yang, A. Li, S. Xiao, R. Cheng, Rapid Removal and Separation of Iron(II) and Manganese(II) from Micropolluted Water Using Magnetic Graphene Oxide, ACS Applied Materials & Interfaces. 6 (2014) 9871-9880.

[69] Z. Abdeen, S.G. Mohammad, M.S. Mahmoud, Adsorption of Mn (II) ion on polyvinyl alcohol/chitosan dry blending from aqueous solution, Environmental Nanotechnology, Monitoring & Management. 3 (2015) 1-9.

[70] Y. Liu, J. Bai, H. Duan, X. Yin, Static magnetic field-assisted synthesis of Fe3O4 nanoparticles and their adsorption of Mn(II) in aqueous solution, Chinese Journal of Chemical Engineering. 25 (2017) 32-36.

[71] X. Zhu, Y. Cui, X. Chang, H. Wang, Selective solid-phase extraction and analysis of trace-level Cr(III), Fe(III), Pb(II), and Mn(II) Ions in wastewater using diethylenetriamine-functionalized carbon nanotubes dispersed in graphene oxide colloids, Talanta. 146 (2016) 358-363.

[72] M. Huang, Y. Zhang, W. Xiang, T. Zhou, X. Wu, J. Mao, Corrigendum to “Efficient adsorption of Mn(II) by layered double hydroxides intercalated with diethylenetriaminepentaacetic acid and the mechanistic study” [J. Environ. Sci. 85 (2019) 56–65], Journal of Environmental Sciences. 90 (2020) 411-412.

[73] Z. Lin, P. Yuan, Y. Yue, Z. Bai, H. Zhu, T. Wang, X. Bao, Selective adsorption of Co(II)/Mn(II) by zeolites from purified terephthalic acid wastewater containing dissolved aromatic organic compounds and metal ions, Science of the Total Environment. 698 (2020) 134287.

[74] R. Mohammadi, A. Azadmehr, A. Maghsoudi, Fabrication of the alginate-combusted coal gangue composite for simultaneous and effective adsorption of Zn(II) and Mn(II), Journal of Environmental Chemical Engineering. 7 (2019) 103494.

[75] S. Lee, D. Tiwari, K. Choi, J. Yang, Y. Chang, H. Lee, Removal of Mn(II) from Aqueous Solutions Using Manganese-Coated Sand Samples, Journal of Chemical & Engineering Data. 54 (2009) 1823-1828.

Figures

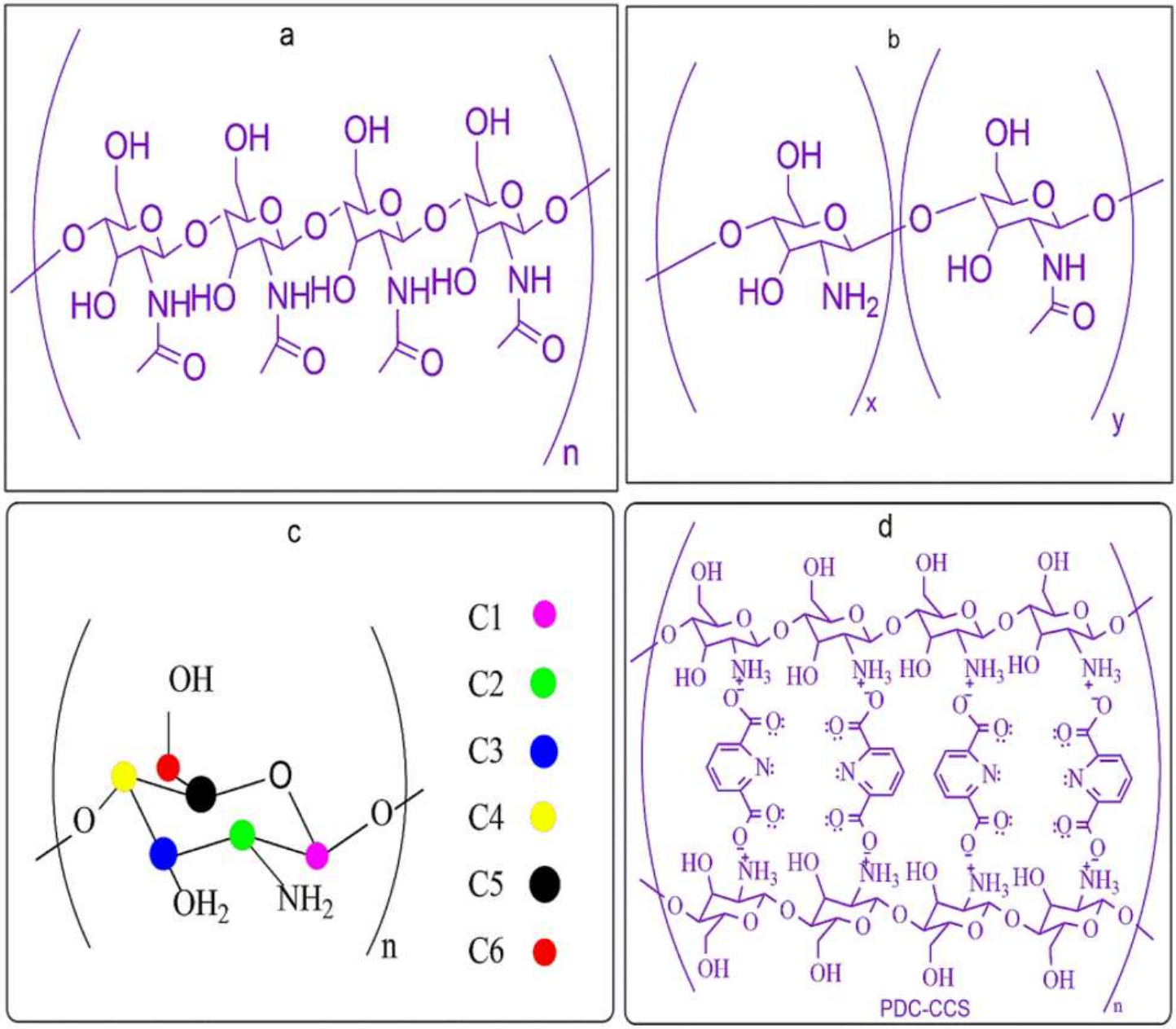

Figure 1

Structure of (a) chitin (b) chitosan (c) fully deacetylated chitosan (d) crosslinked chitosan showing possible binding sites

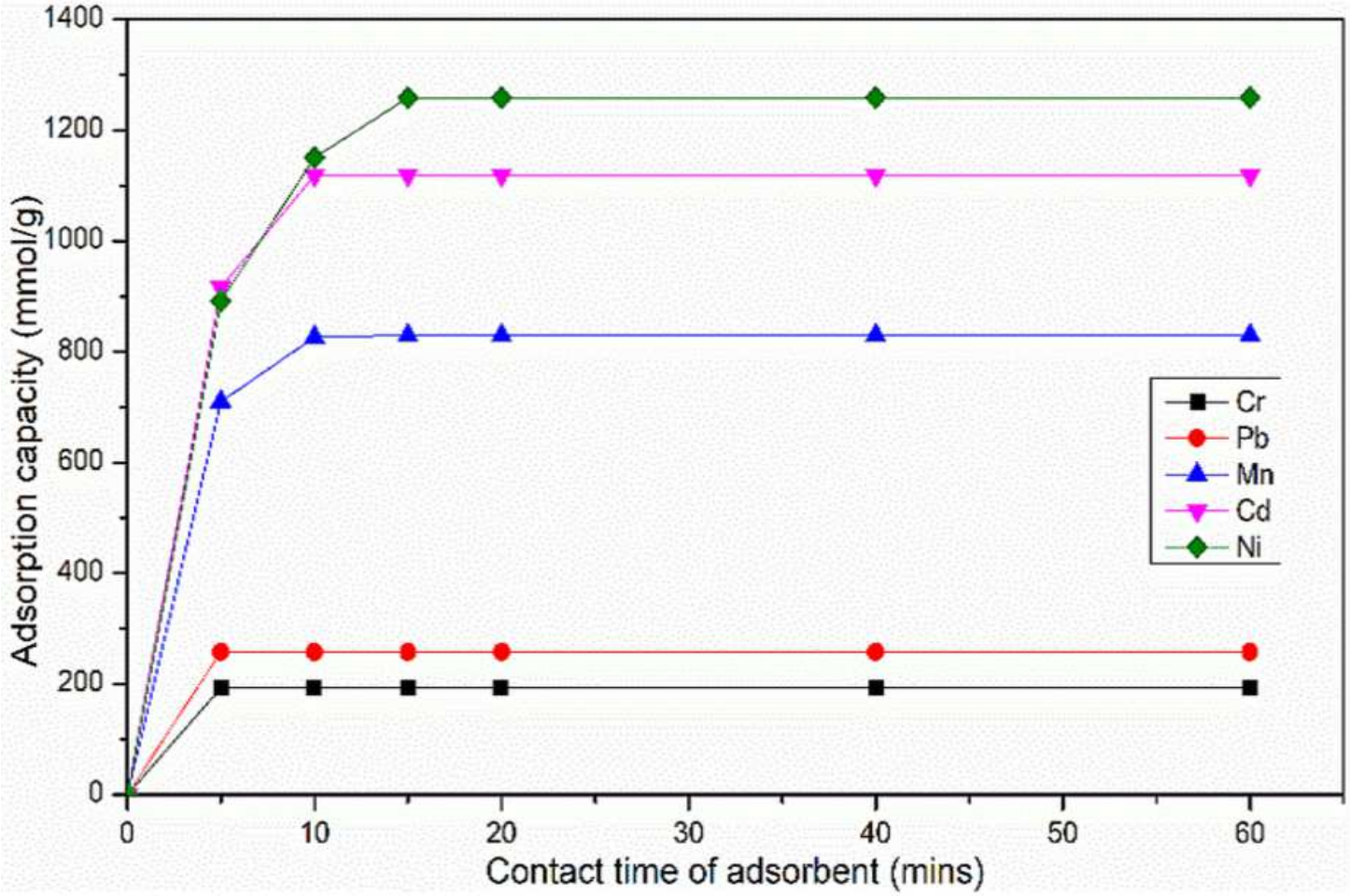

Figure 2

Capacity of adsorption of PDC-CCS for Cr3+, Pb2+, Mn2+, Cd2+, and Ni2+ [at 30 ℃, pH 7.5, initial metal ion concentration of 2.5 mmol/l]

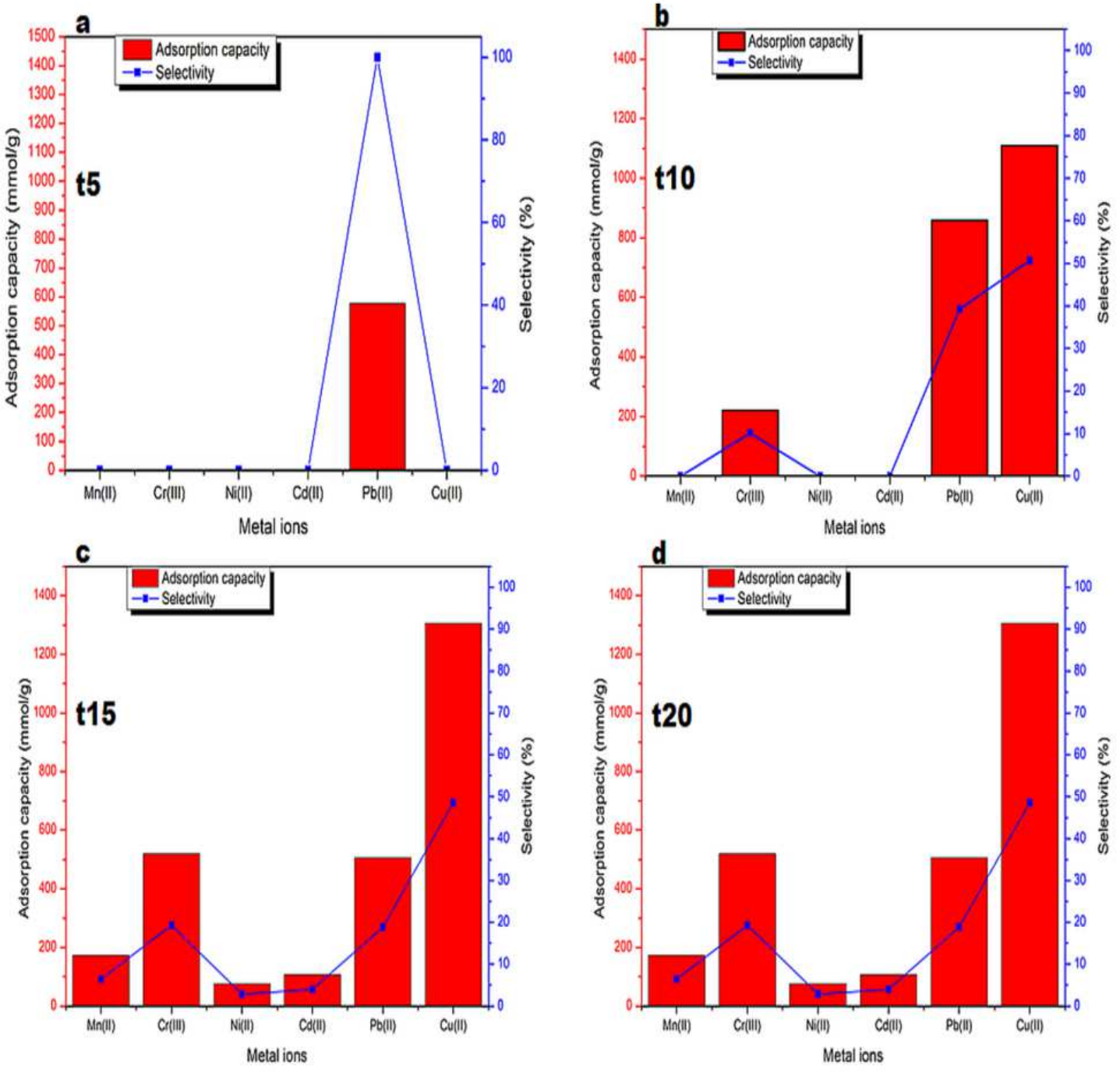

Figure 3

Competitive adsorption capacities and selectivity of PDC-CCS at pH 4.2 for Mn2+, Cr3+, Ni2+, Cd2+, Pb2+, and Cu2+ within; (a) five mins (b) ten mins (c) fifteen mins and (d) twenty mins.

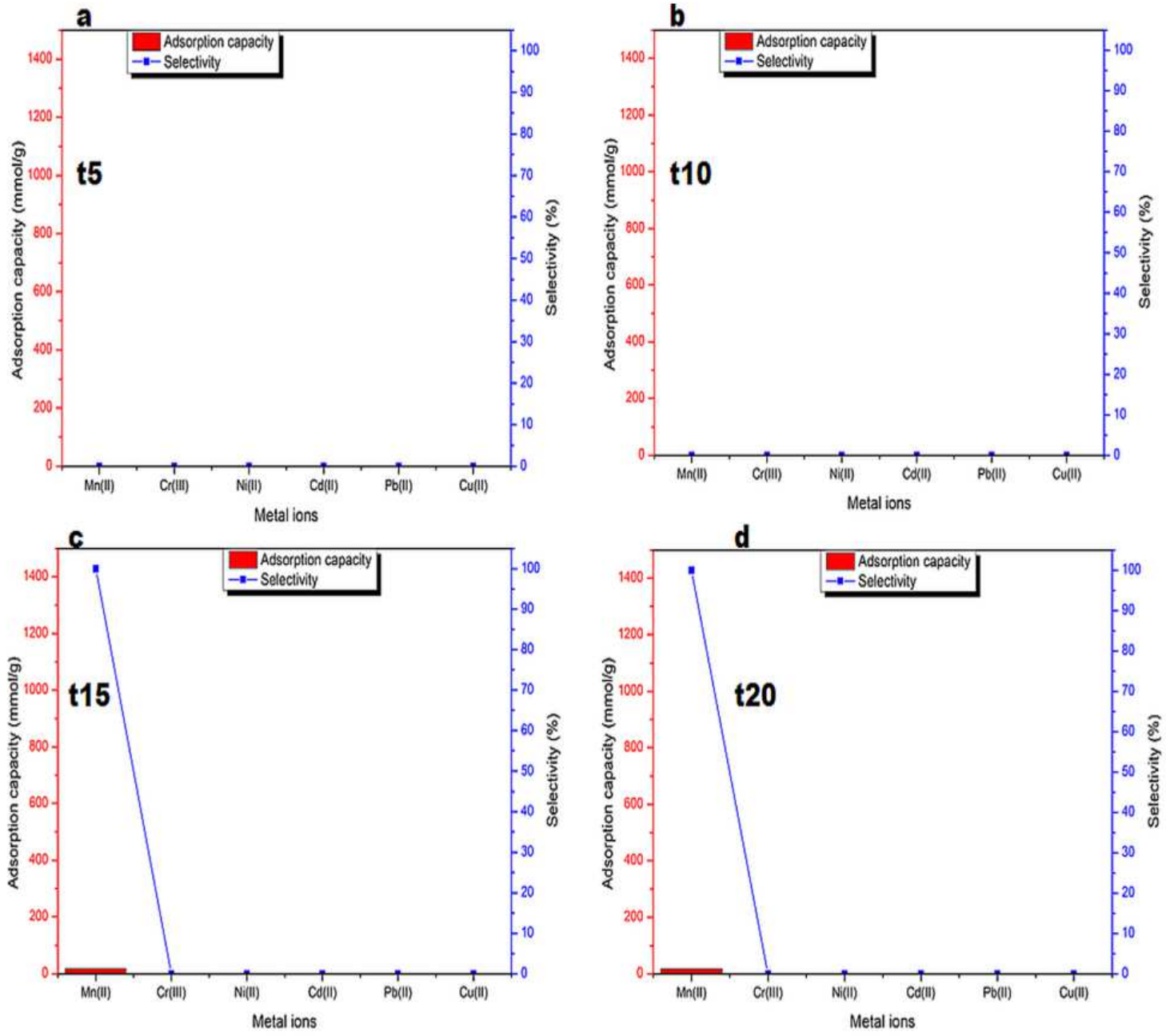

Figure 4

Competitive adsorption capacities and selectivity of PDC-CCS at pH 5.6 for Mn2+, Cr3+, Ni2+, Cd2+, Pb2+, and Cu2+ within; (a) five mins (b) ten mins (c) fifteen mins and (d) twenty mins.

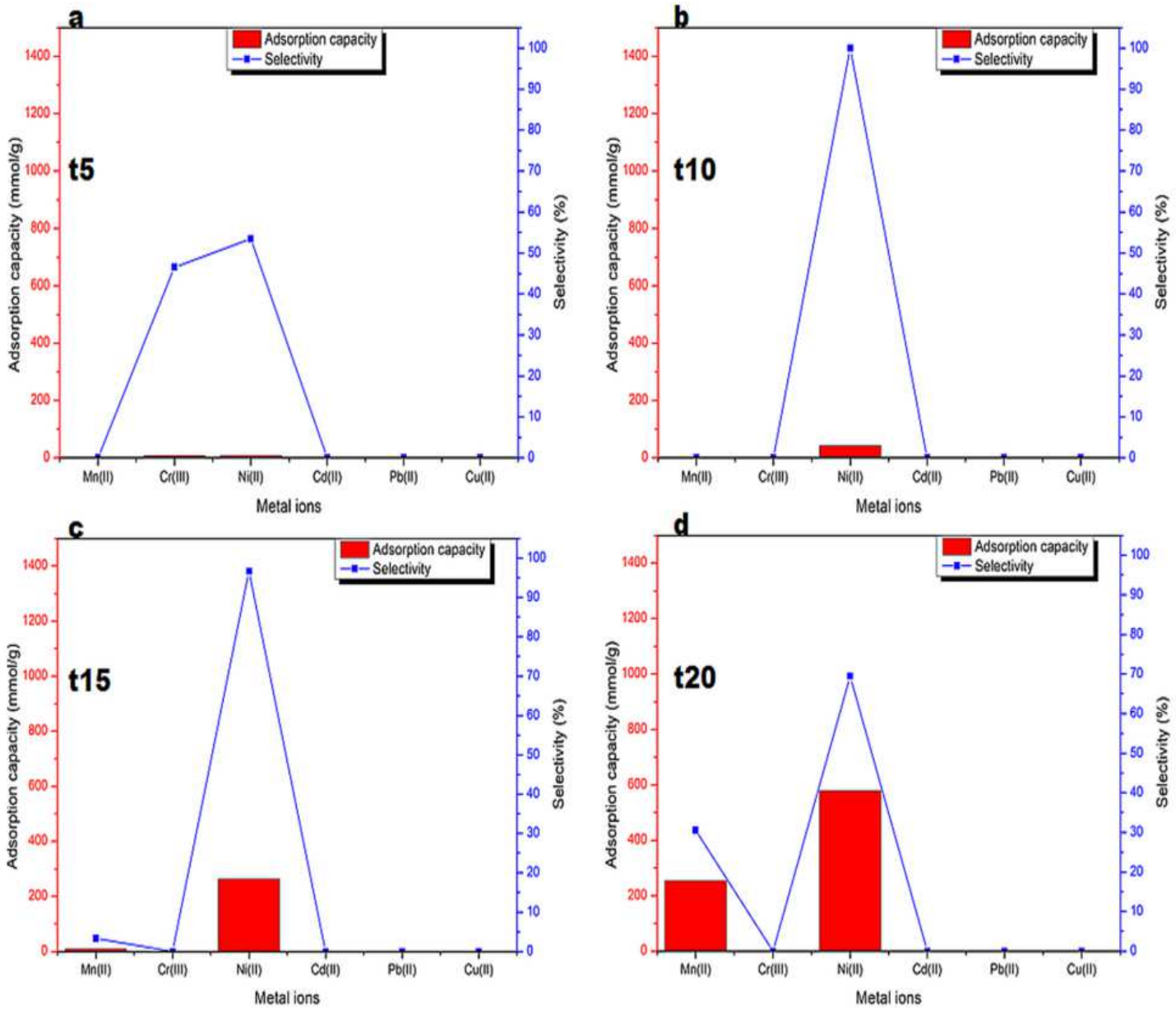

Figure 5

Competitive adsorption capacities and selectivity of PDC-CCS at pH 6.65 for Mn2+, Cr3+, Ni2+, Cd2+, Pb2+, and Cu2+ within; (a) five mins (b) ten mins (c) fifteen mins and (d) twenty mins.

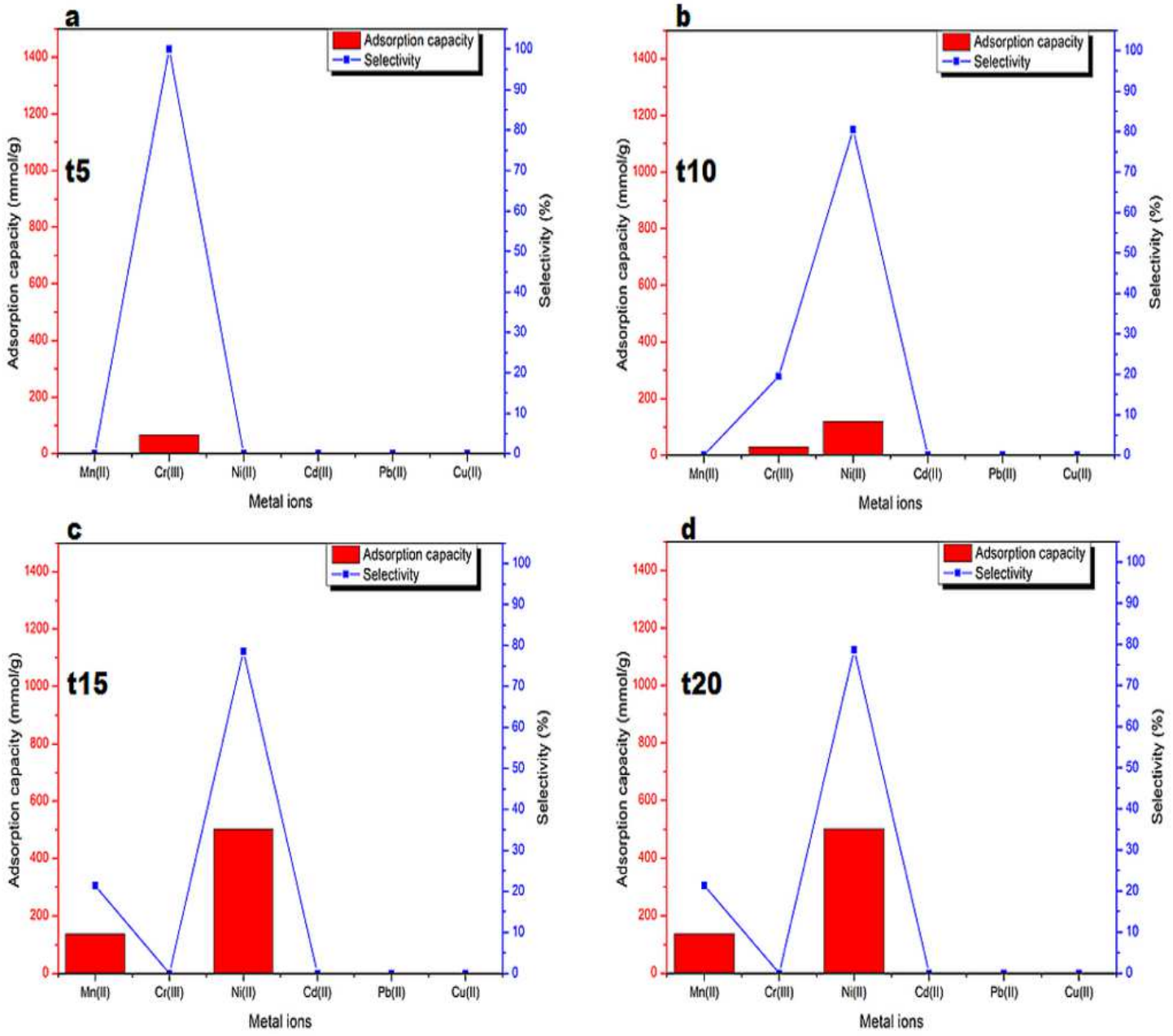

Figure 6

Competitive adsorption capacities and selectivity of PDC-CCS at pH 7.61 for Mn2+, Cr3+, Ni2+, Cd2+, Pb2+, and Cu2+ within; (a) five mins (b) ten mins (c) fifteen mins and (d) twenty mins.

Supplementary Files

This is a list of supplementary files associated with this preprint. Click to download.

- GraphicalabstractP32.tif
- Supplementaryinformation.docx